*Journal of Chromatography*, 205 (1981) 239–249
Elsevier Scientific Publishing Company, Amsterdam — Printed in The Netherlands

CHROM. 13,360

# LIQUID CRYSTALS AS STATIONARY PHASES IN GAS–LIQUID CHROMATOGRAPHY

## III. THERMODYNAMIC MEASUREMENTS ON DECANE–DIHEXYLOXYAZOXYBENZENE AND DECANE–DIHEPTYLOXYAZOXYBENZENE SYSTEMS

J. F. BOCQUET and C. POMMIER*

*Centre Scientifique et Polytechnique, Laboratoire de Chimie Physique, E.R.A. C.N.R.S. 456, 93430 Villetaneuse (France)*

(First received July 9th, 1980; revised manuscript received September 22nd, 1980)

SUMMARY

Gas–liquid chromatography at finite solute concentration has been used to determine distribution isotherms, phase diagrams and solute thermodynamic functions in decane–dihexyloxyazoxybenzene and decane–diheptyloxyazoxybenzene systems. A complete interpretation of the anomalous elution peak profiles of large samples is given, and the influence of the pressure gradient in the column has been investigated.

## INTRODUCTION

The thermodynamics of solutions of a non-mesomorphic solute in a liquid crystal have extensively been studied at infinite dilution by several authors[1–5] using gas–liquid chromatography (GLC). We have used the same technique to investigate the influence of the solute concentration on the properties of such solutions.

In previous papers[6,7] we reported anomalous elution peak profiles obtained when large amounts of sample are injected in a chromatographic column containing a nematic liquid crystal as stationary phase. These profiles (Fig. 1b) observed below the clarification temperature of the liquid crystal have been discussed in terms of discontinuous distribution isotherms: for the studied system, a particular gas phase solute concentration, $C_t^G$, is in equilibrium with two different liquid phase solute concentrations, $C^N$ and $C^I$, in a nematic and an isotropic phase respectively. This hypothesis of reversible destruction of the order in the stationary phase in the course of elution has been confirmed by a comparison between experimental peaks and those obtained from simulation of the propagation of a solute plug through the chromatographic column using plate theory[7]. Furthermore, when a large amount of solute is eluted by a carrier gas containing a given concentration of the same solute, a "step" is observed on the rear peak profile (Fig. 2). We have shown that the gas phase concentration of this "step" is $C_t^G$.

Fig. 1 shows the comparison between an experimental elution peak and a

0021-9673/81/0000–0000/$02.50 

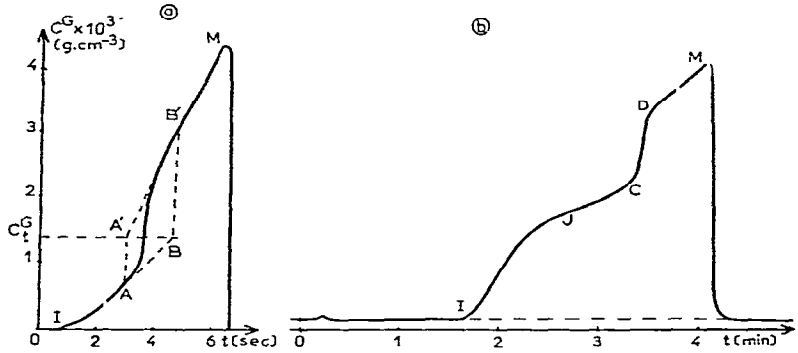


Fig. 1. Comparison between simulated (a) and experimental (b) peaks; a, simulation from isotherm in Fig. 4a; b, 10 $\mu$l of decane injected on DHAB, $T = 121.1$°C.

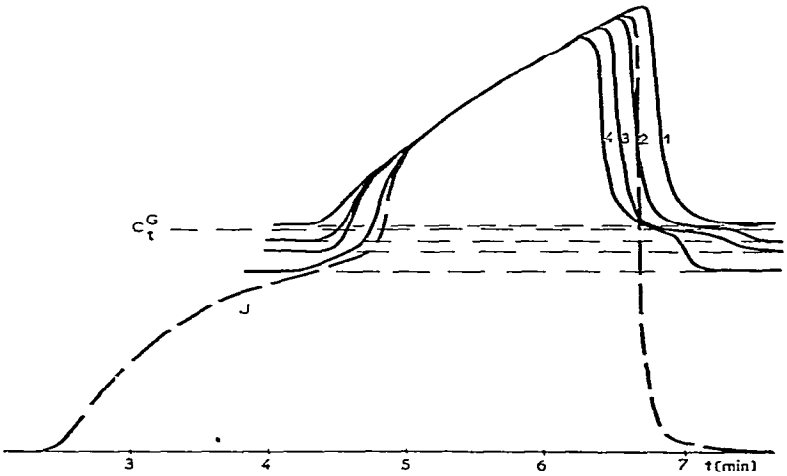


Fig. 2. Peak profiles obtained by elution with a carrier gas containing various solute concentrations (injection, 5 $\mu$l; $T = 121.1$°C). Decane concentration in helium ($\times 10^5$ g cm$^{-3}$): 1, 15.3; 2, 14.3; 3, 13.6; 4, 12.0. – – –, Elution of 15 $\mu$l of decane by pure helium.

simulated peak obtained from an anti-Langmuir discontinuous isotherm (Fig. 4a). For low solute concentrations (IJ, IA) and high solute concentrations (DM, B'M) the two peaks are in accordance. So, these parts correspond to retentions on a nematic and an isotropic phase respectively. Nevertheless, the JC part of the experimental peak cannot be directly related to any part of the distribution isotherm. Fig. 3 compares the retention volumes of various solute concentrations obtained by large sample elution and by step and pulse chromatography under the same conditions of column pressure drop and temperature. The agreement is quite good and, moreover, it can be seen that the A'D part of the isotherm is attainable by the second method.

In the present paper we shall complete the theoretical treatment of this phenomenon by studying the effect of the pressure drop in the column. Then a direct determination of $C_t^G$ from a single large sample elution peak is proposed. Distribution

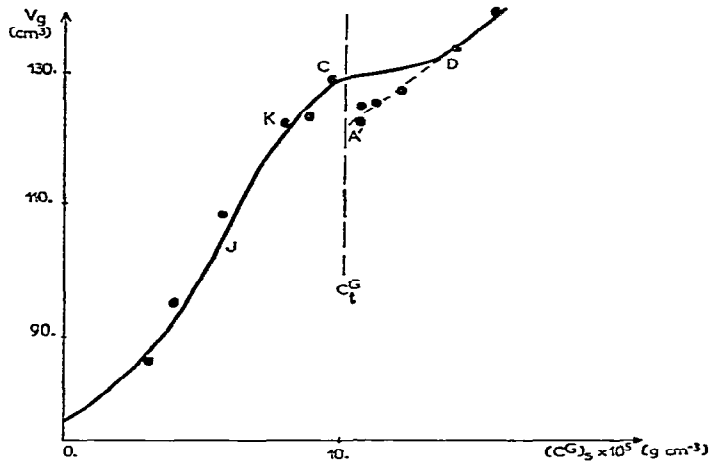


Fig. 3. Comparison between large sample elution profile (—) and step and pulse chromatography (●). System: $C_{10}H_{22}$–DHAB; $T = 124.4°C$; $\Delta P = 620$ mmHg.

isotherms, thermodynamic parameters (solute activity coefficient, solute molar excess enthalpies and entropies) and phase diagrams in the systems decane–dihexyloxyazoxybenzene (DHAB) and decane–diheptyloxyazoxybenzene (PHAB) are determined.

## EXPERIMENTAL

DHAB and PHAB (E. Merck, Darmstadt, G.F.R.) were recrystallized three times in ethanol before use. The transition temperatures were determined by calorimetry:

for DHAB

$$\text{crystal} \xrightarrow{81°C} \underset{\text{liquid}}{\text{nematic}} \xrightarrow{129.7°C} \underset{\text{liquid}}{\text{isotropic}}$$

for PHAB

$$\text{crystal} \xrightarrow{70°C} \underset{\text{liquid}}{\text{smectic}} \xrightarrow{93.7°C} \underset{\text{liquid}}{\text{nematic}} \xrightarrow{123.3°C} \underset{\text{liquid}}{\text{isotropic}}$$

Decane (Carlo Erba, Milan, Italy) is a pure compound for chromatography.

The chromatograph was a Model Girdel 3000 (Giravions Dorand, Suresnes, France) equipped with an oil-bath, the temperature of which is regulated within 0.1°C. The columns (0.8–2 m × 2 mm I.D.) were filled with Chromosorb W AW DMCS (60–80 mesh) coated 15% by weight with the liquid crystal. The flow-rate of the carrier gas (helium) was 5–20 $cm^3\ min^{-1}$.

Differential calorimetric experiments were performed with a MCB calorimeter (Arion, Grenoble, France). The heating rate was $0.5°K\ min^{-1}$.

The vapor pressure measurements were made with a Barocel vacuum sensor (Datametrics, Wilmington, DE, U.S.A.). The sensing element was a high-precision capacitive potentiometer and the variable element was a thin metal diaphragm between two enclosures, one connected to the vacuum line, the other to the sample cell.

## RESULTS

*Influence of the pressure drop in the column*

For the studied solute (decane) and under the experimental conditions (temperature, solute concentrations) we can consider that the retention process is essentially governed by dissolution effects; the sorption effect may be neglected.

Fig. 4a shows the distribution isotherm used in order to obtain simulated peaks similar to experimental ones (Fig. 1). The two liquid phase concentrations, A′ and B, travel at different rates in the column and $K''_{A'}$ must be lower than $K''_{B}$ (ref. 7) ($K''$ is the slope $\partial C^{L}/\partial C^{G}$, where $C^{L}$ and $C^{G}$ are expressed in grams of solute per gram of liquid phase and in grams of solute per cm³ of gas phase respectively). Under these conditions Fig. 4a′ represents the elution peak obtained on a column without pressure gradient. The concentrations A and A′ have the same $K''$ values. The A′D and AB parts cannot be observed on the peak profile. However, in a real column a pressure gradient exists. A gas solute concentration, $C_0^G$, on the chromatogram (recorded at the

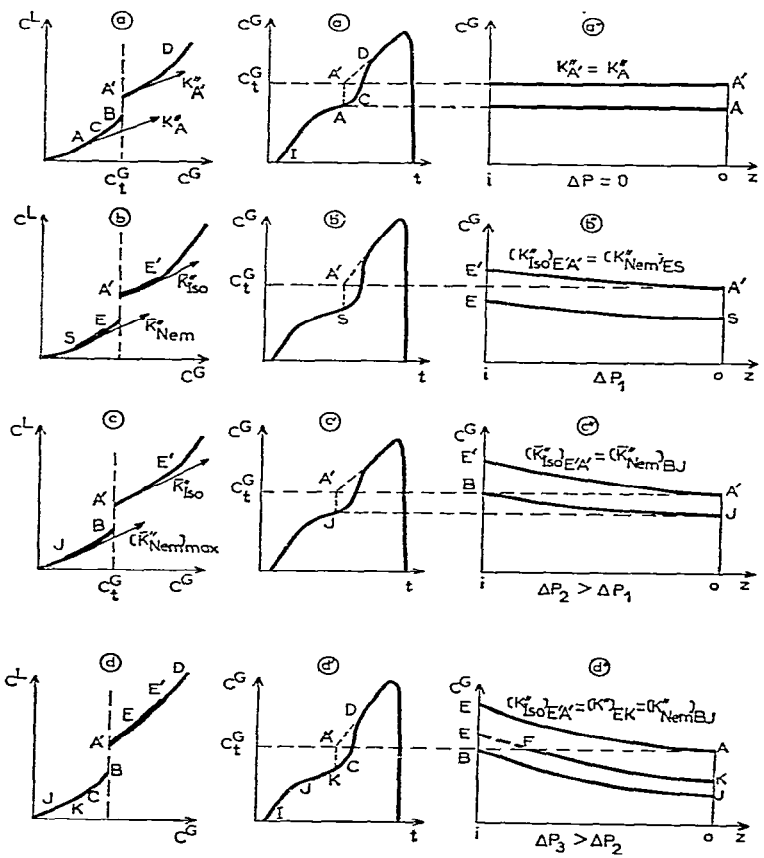


Fig. 4. Influence of the pressure gradient in the column on the front peak profile: a, b, c, d = distribution isotherm; a′, b′, c′, d′ = expected peak profile; a″, b″, c″, d″ = evolution of solute concentration through the column.

outlet pressure, $P_0$) corresponds to an inlet gas solute concentration, $C_i^G$. These are related by the expression:

$$C_i^G/C_0^G = P_i/P_0 \quad (1)$$

So, a mean value of $K''$ ($\bar{K}''$) between $K''$ ($C_i^G$) and $K''$ ($C_0^G$) will be associated with $C_0^G$. Under these conditions and for a weak pressure gradient ($P_i - P_0 = \Delta P_1$), the retention time of the point A' extrapolated on the chromatogram (Fig. 4b') will be proportional to $K''_{Iso}$ which is associated with the A'E' arc (Fig. 4b). On the nematic part of the isotherm, there will exist an arc SE for which $\bar{K}''_{Iso} = \bar{K}''_{Nem}$. Point E is between A and B, the position of S depending on the curvature of each part of the isotherm. On the chromatogram (Fig. 4b') the retention time of A' is greater than in the previous case without pressure drop ($\bar{K}''_{Iso}$ is greater than $\bar{K}''_{A'}$). For a greater pressure gradient in the column, the arcs A'E' and ES increase, as does the retention time of A'. For the value $\Delta P_2$ (Fig. 4c, c', c''), points E and S reach B and J respectively. For a pressure gradient $\Delta P_3$ greater than $\Delta P_2$ (Fig. 4d, d', d''), the largest possible value of $\bar{K}''_{Nem}$ (JB) will be lower than $\bar{K}''_{Iso}$ (A'E'). This means that for outlet concentrations between J and C the solute has been retained on an isotropic phase in the first part of the column, and on a nematic phase in the last part. Then, J will appear as a singular point on the front peak profile and its gas phase concentration can be related to $C_t^G$ by the relation:

$$C_B^G/C_J^G = C_t^G/C_J^G = P_i/P_0 \quad (2)$$

In Table I are reported the $C_t^G$ values obtained from eqn. 2 and from elution of large samples by carrier gas containing a known concentration of solute[7]. There is a good agreement between the two methods.

TABLE I

DETERMINATION OF THE GAS PHASE CONCENTRATION, $C_t^G$

System: DHAB–decane; $T = 121.1$°C.

| *Step-and-pulse chromatography* | | *Large sample elution* | |
|---|---|---|---|
| *ΔP (mmHg)* | $C_t^G \times 10^5$ *(g cm$^{-3}$)* | *ΔP (mmHg)* | $C_t^G \times 10^5$ *(g cm$^{-3}$)* |
| 121 | 15.69 | 65 | 15.38 |
| 330 | 15.16 | 86 | 15.1 |
| 333 | 15.05 | 106 | 15.29 |
| 354 | 15.22 | 479 | 15.72 |
| 539 | 15.38 | 514 | 15.45 |
| 549 | 15.69 | 764 | 15.78 |
| Mean: | 15.3 ± 0.3 | Mean: | 15.4 ± 0.4 |

The influence of the pressure drop in the column is clearly shown in Fig. 5 where the difference between the specific retention volumes $(V_g)_{A'} - (V_g)_J$ is plotted *versus* $\Delta P$. The retention times of the points A' and J are different above $\Delta P \approx 50$ mmHg. Because of the curvature of the two parts of the isotherm, the propagation rate of points C and D may be different. If so, the discontinuity CD is not completely stable

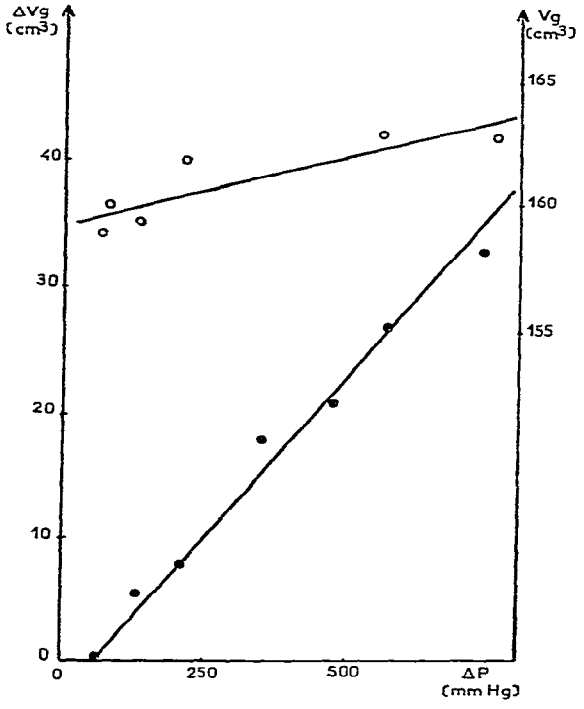


Fig. 5. Influence of the pressure gradient on $\Delta V_g = (V_g)_{A'} - (V_g)_J$ (●), and on the retention volume of the discontinuity CD (○).

and the retention time of the mean point of this discontinuity must be a function of the pressure gradient. Fig. 5 shows that this function is very smooth so that the curvatures of the two parts of the isotherm on both sides of $C_t^G$ are very similar.

*Determination of the distribution isotherms*

The isotherms are defined as the curves $C^L = f(C^G)$. Because of the pressure drop in the column, each point of the front profile will be associated with a mean concentration $\bar{C}^G = J_3^4 C_0^G$ and with a mean capacity ratio, $\bar{K}''$, which is proportional to the retention time $t_R$. From $\bar{K}''$ and $C^G$, calculation of $C^L$ necessitates an integration from $\bar{C}^G = 0$ to $\bar{C}^G$. So, the isotropic part of the profile must be extrapolated to $\bar{C}^G = 0$. We have extrapolated the linear relationship $\ln V_g = f(1/T)$ at infinite dilution experimentally observed at $T > T_c$ down to lower temperatures. Then, the distribution isotherms have been determined from large sample elution peaks as follows.

1. The front profile has been corrected for diffusion;
2. Concentration $C_t^G$ has been calculated from eqn. 2;
3. The profile has been expressed in terms of mean values, $\bar{C}^G$;
4. The nematic and isotropic parts have been extrapolated up to $C_t^G$ and down to $\bar{C}^G = 0$ respectively;
5. For a given point, the $\bar{C}^L$ value has been determined by integration of the function $\bar{K}'' = f(\bar{C}^G)$.

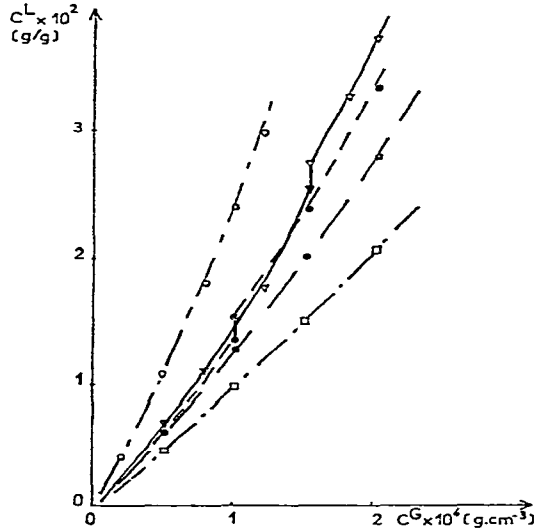


Fig. 6. Distribution isotherms for the system $C_{10}H_{22}$–DHAB: ○, 100°C; ▽, 121.1°C; ●, 124.4°C; ◐, 130.6°C; □, 141.8°C.

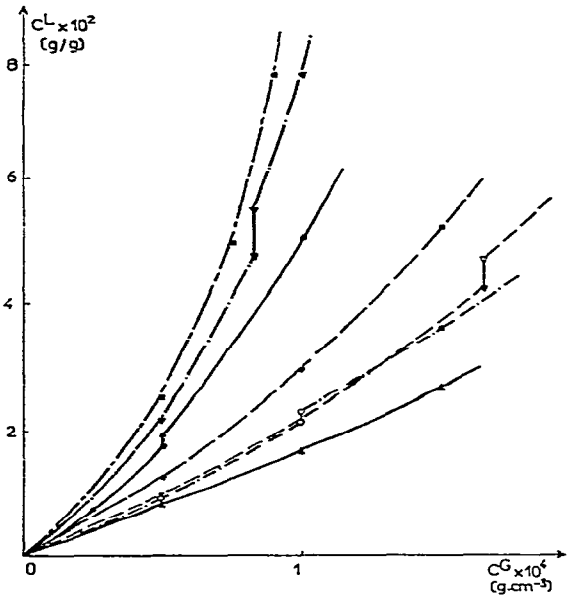


Fig. 7. Distribution isotherms for the system $C_{10}H_{22}$–PHAB: ■, 75°C; ▼, 80°C; ◐, 88.3°C; ●, 102.6°C; ▽, 113.1°C; ○, 118°C; ▲, 128°C.

Fig. 6 shows selected distribution isotherms for five temperatures for the system decane–DHAB. At 121.1°C and 124.4°C there is a discontinuity in $C^L$ (this had not been noticed in our first paper[6]). For PHAB such discontinuities are observed both at the nematic–isotropic phase transition and at the smectic–nematic phase transition (Fig. 7).

*Phase diagrams*

The knowledge of the distribution isotherms allows us to determine directly the phase diagrams of the studied systems. For any temperature we can obtain the concentrations $C^N$ and $C^I$ of the two liquid phases in equilibrium with the gas phase of concentration $C_t^G$. However, the determination of the limits of the two-phase domain is less precise for low and high solute concentrations in the liquid phase. Just below the clarification temperature, a small error in the determination of $C_t^G$ will lead to large errors in the liquid phase solute concentration. In the same way, for low temperatures, interpolation of the isotropic profile between the experimental part and the retention time at infinite dilution becomes less precise. In the mole fraction range $0.03 < X_2^L < 0.15$ the relative error in $X_2^N$ and $X_2^I$ is estimated to be 2%. Moreover, in order to obtain the isotropic part of the chromatogram, large quantities of solute must be injected; this may lead to migration of the stationary phase through the column. We have verified that this phenomenon does not occur up to a solute mole fraction equal to 0.2 in the liquid phase. The phase diagrams are shown in Fig. 8. The limits of the two-phase domain can be assimilated as straight lines in each case.

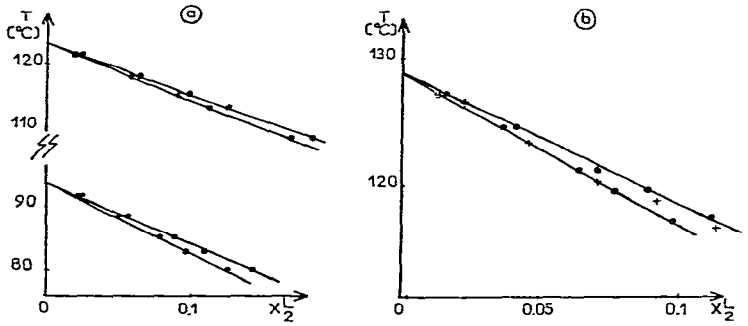


Fig. 8. Phase diagrams: a, $C_{10}H_{22}$–PHAB; b, $C_{10}H_{22}$–DHAB; +, calorimetric results.

The determination of the phase diagrams by GLC is very indirect and we have tested this method by comparing the results with those obtained by calorimetric measurements for the decane–DHAB system. The significance of the singular points on the thermograms has been explained elsewhere[6]. We have plotted in Fig. 8b the temperatures of commencement of the two-phase domain. Owing to the weak thermal conductivity of the samples, the temperature of the end of the transition cannot be determined. However, there is good agreement between the two methods.

*Activity coefficients*

Activity coefficients are determined from the isotherms by the classical thermodynamical relation

$$\gamma_2 = \frac{X_2^G \bar{P}}{X_2^L P_2^\circ} \cdot \exp\left[\frac{(B_{22} - V_2^\circ)(\bar{P} - P_2^\circ)}{RT} + \frac{\delta(1 - X_2^G)^2 \bar{P}}{RT}\right] \qquad (3)$$

where $X_2^G$ and $X_2^L$ are the solute mole fractions in the gas phase and in the liquid phase respectively, $\bar{P} = J_3^4 P_0$ is the mean pressure in the column, $P^\circ$ and $V_2^\circ$ are the vapour

pressure and molar volume of the pure solute and $\delta = 2B_{23} - B_{22} - B_{33}$ where $B_{ij}$ are the virial coefficients (2, solute; 3, carrier gas). The carrier gas is helium, so we shall assume that $B_{23}$ and $B_{33}$ are equal to zero. The $B_{22}$ values have been calculated from literature data[8].

Plots of $\ln \gamma_2$ *versus* $1/T$ for various values of $C^L$ are shown in Figs. 9 and 10. These variations must be linear if the dissolution enthalpies, $\overline{H}_2^c$, are independent of temperature. This evolution (*i.e.*, the linear variation of $\ln \gamma$ *vs.* $1/T$) is observed experimentally for the isotropic phase and the nematic phase out of the pretransition domain. The pretransition effects decrease the activity coefficient in a range of about 15°C below the transition temperature. At finite dilution of solute, this phenomenon

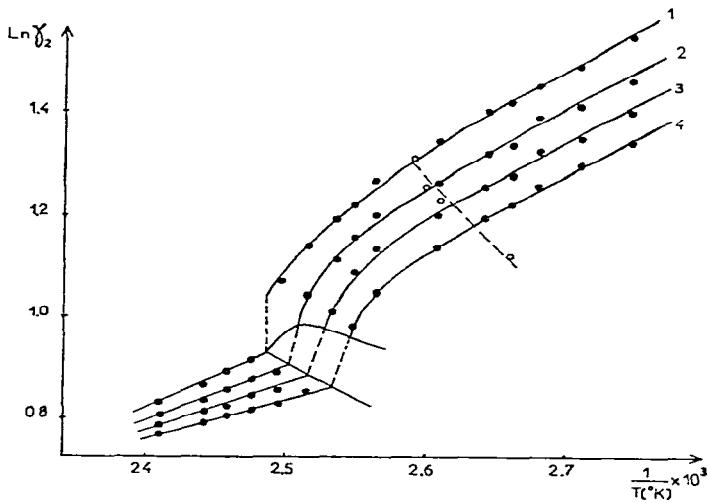


Fig. 9. Decane activity coefficient in DHAB for selected concentrations: 1, infinite dilution; 2, $C_2^L = 1 \cdot 10^{-2}$ g/g; 3, $C_2^L = 2 \cdot 10^{-2}$ g/g; 4, $C_2^L = 3 \cdot 10^{-2}$ g/g; ○, calorimetric results.

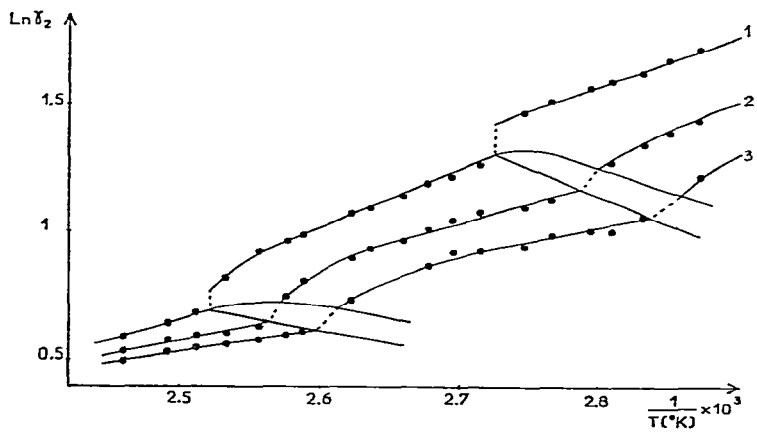


Fig. 10. Decane activity coefficients in PHAB for selected concentrations: 1, infinite dilution; 2, $C_2^L = 3 \cdot 10^{-2}$ g/g; 3, $C_2^L = 6 \cdot 10^{-2}$ g/g.

is very weak near the smectic–nematic phase transition. A discontinuity in $\ln \gamma_2$ is observed for each curve. For a finite solute concentration, this discontinuity occurs at the two temperatures limiting the two phase domain.

In Table II are shown the values of the partial molar excess enthalpies and entropies in the liquid phases of DHAB and PHAB for various decane concentrations. The values for the system decane–DHAB are slightly different from those reported in a previous paper[6] because of a larger number of experimental points in the present work.

We have tested the validity of the GLC measurements, comparing these results with those obtained by a static method. Decane activity coefficients have been determined by vapour pressure measurements. In this case, $\gamma_2$ can be directly calculated from

TABLE II

EXCESS FUNCTIONS OF DECANE IN DHAB AND PHAB

($\bar{H}_2^e$ are in kcal mole$^{-1}$; $\bar{S}_2^e$ are in cal mole$^{-1}$ °K$^{-1}$.

| | $X^L$ | $(\bar{H}_2^e)^S$ | $(\bar{S}_2^e)^S$ | $(\bar{H}_2^e)^N$ | $(\bar{S}_2^e)^N$ | $(\bar{H}_2^e)^I$ | $(\bar{S}_2^e)^I$ |
|---|---|---|---|---|---|---|---|
| DHAB | Infinite dilution | — | — | 3.12 ± 0.07 | 5.48 ± 0.17 | 2.51 ± 0.07 | 4.39 ± 0.17 |
| | 0.027 | — | — | 2.86 ± 0.1 | 4.95 ± 0.26 | 2.08 ± 0.07 | 3.41 ± 0.17 |
| | 0.053 | — | — | 2.78 ± 0.15 | 4.85 ± 0.41 | 1.83 ± 0.08 | 2.84 ± 0.20 |
| | 0.077 | — | — | 2.68 ± 0.15 | 4.69 ± 0.41 | 1.54 ± 0.07 | 2.19 ± 0.17 |
| PHAB | Infinite dilution | 3.86 ± 0.07 | 7.68 ± 0.19 | 4.46 ± 0.10 | 9.61 ± 0.27 | 3.04 ± 0.09 | 6.32 ± 0.22 |
| | 0.082 | — | — | 3.04 ± 0.20 | 6.16 ± 0.53 | 2.14 ± 0.07 | 4.21 ± 0.17 |
| | 0.152 | — | — | 2.23 ± 0.25 | 4.25 ± 0.7 | 1.69 ± 0.1 | 3.16 ± 0.26 |

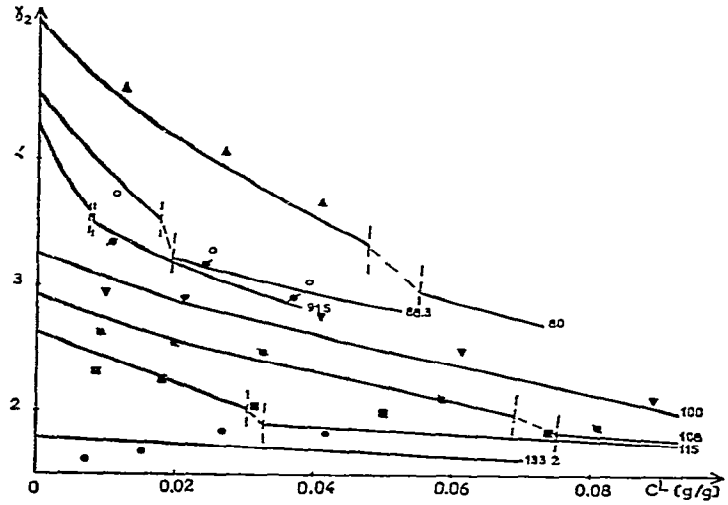


Fig. 11. Comparison between GLC results (—) and vapour pressure measurements for $C_{10}H_{22}$–PHAB system: ▲, 80°C; ○, 88.3°C; ◪, 91.5°C; ▼, 100°C; ◪, 108°C; ■, 115°C, ●, 133.2°C.

eqn. 3 in which the second term of the exponential is zero, and $X_2^G\bar{P}$ is the measured pressure. The values obtained for the system decane–PHAB are compared with the GLC results in Fig. 11. The agreement is good; however, the points obtained by vapour pressure measurements are rather scattered and the limits of the two-phase domain are imprecise. The use of a vacuum microbalance system would allow a more accurate determination of the domain[9].

## CONCLUSION

The gas chromatographic method proposed is of interest in determining the thermodynamic properties of a non-mesamorphic solute dissolved in a liquid crystal, as well as a part of the phase diagram of the system. This method is fast and easy to perform. The accuracy of the results is of the same order as for classical methods such as thermal analysis and vapour pressure measurements. In the present work, with decane as solute, sorption effects have been neglected in the retention process. However, with more volatile solutes, these effects will be larger and cannot be neglected. In the following paper[10], we compare the behaviour of such solutes having different molecular shapes, benzene and carbon tetrachloride.

## REFERENCES

1 G. A. Oweimreen, G. C. Lin and D. E. Martire, *J. Phys. Chem.*, 83 (1979) 2111.
2 D. E. Martire, A. Nikolić and K. L. Vasanth, *J. Chromatogr.*, 178 (1979) 401.
3 D. G. Willey and G. H. Brown, *J. Phys. Chem.*, 76 (1972) 99.
4 A. Jeknavorian, P. Barrett, A. C. Watterson and E. F. Barry, *J. Chromatogr.*, 107 (1975) 317.
5 G. Kraus, K. Seifert and H. Schubert, *J. Chromatogr.*, 100 (1974) 101.
6 J. F. Bocquet and C. Pommier, *J. Chromatogr.*, 117 (1976) 315.
7 J. F. Bocquet and C. Pommier, *J. Chromatogr.*, 166 (1978) 357.
8 M. L. Mac Glashan and D. J. B. Potter, *Proc. R. Soc. London, Ser. A*, 267 (1962) 478.
9 H. T. Peterson and D. E. Martire, *Mol. Cryst. Liq. Cryst.*, 25 (1974) 89.
10 J. F. Bocquet and C. Pommier, *J. Chromatogr.*, 205 (1981) 251.